Forest Ecology and Management 458 (2020) 117798

Contents lists available at ScienceDirect

Forest Ecology and Management

journal homepage: www.elsevier.com/locate/foreco

Savanna vegetation structure in the Brazilian Cerrado allows for the accurate estimation of aboveground biomass using terrestrial laser scanning

Barbara Zimbres[a,b,*], Julia Shimbo[b], Mercedes Bustamante[a], Shaun Levick[c], Sabrina Miranda[d], Iris Roitman[b], Divino Silvério[b], Leticia Gomes[a], Christopher Fagg[e], Ane Alencar[b]

[a] Ecology Department, University of Brasilia, Campus Darcy Ribeiro, Brasilia 70910-900, Brazil
[b] Amazon Environmental Research Institute (IPAM), SCN 211, bloco B, sala 201, Brasilia 70836-520, Brazil
[c] Tropical Ecosystems Research Centre, CSIRO Land and Water, 564 Vanderlin Dr, Berrimah, NT 0828, Australia
[d] Goiás State University, Rua S-7 s/n Bairro Sul, Palmeiras de Goiás 76190-000, Brazil
[e] Ceilandia College, University of Brasilia, Centro Metropolitano, Ceilândia Sul, Brasilia 72220-275, Brazil

ARTICLE INFO

Keywords:
Allometric equation
Forest
Terrestrial LiDAR
TLS
Carbon stock
Three-dimensional model

ABSTRACT

Understanding structural variations in natural systems can help us understand their responses to disturbance and environmental changes and plan for the mitigation of human-induced impacts. Terrestrial laser scanning (TLS) is a technological solution to quickly and accurately capture and model vegetation structure. In the Brazilian Cerrado biome, characterized by highly heterogeneous plant formations and marked seasonality, TLS may help improve aboveground biomass (AGB) estimates. This study aimed to use single-scan TLS-derived metrics to predict plot-scale aboveground biomass for three vegetation types with high structural diversity and biomass content (woodland savanna, forested savanna, and gallery forest). Ten plots were scanned in each vegetation type, and variables related to point density at different strata and height distribution were extracted from the point cloud to predict AGB measured in local field inventories. The woodland savanna provided good fit models with only two metrics (rainy season: proportion of points below 1.37 m and height of the 99th percentile; adj-R^2 = 0.92, RMSE (root mean square error) = 2.67 Mg/ha or 12%; and dry season: height of the 20th and the 99th percentiles; adj-R^2 = 0.88, RMSE = 3.32 Mg/ha or 15%). The model for the forested savanna had relatively less explanatory power with one influential predictor (forested savanna: height of the 20th percentile; adj-R^2 = 0.58, RMSE = 6.85 Mg/ha or 21%). For the gallery forest, however, the canopy structure could not be adequately characterized due to occlusion of laser returns by dense sub-canopy strata. Our study shows the strong potential of the terrestrial LiDAR technology for estimation of plot-based biomass across diverse savanna vegetation types, where the sparse tree structure allows for better laser penetration the accurate generation of height profiles.

1. Introduction

The natural and anthropogenic-driven variations in the structure of natural systems are a key object of study in Ecology. They shed light not only in the natural dynamics that take place in these systems, but help us to understand and plan for the mitigation of human-induced impacts in a changing world. For example, the monitoring of vegetation structure in terms of biomass will allow for the estimation of carbon stock variations and greenhouse gas emissions caused by forest loss and degradation in the context of land use and climate change (Ciais et al., 2013; Asner et al., 2010; Dixon et al., 1994). Ecosystem processes, as well as biodiversity patterns, can also be indirectly inferred from the assessment of vegetation structure, and descriptors of structure and biomass have often been applied as proxies for a myriad of natural patterns and processes (Blakey et al., 2017; Froidevaux et al., 2016; Jenkins, 2015; Vilà et al., 2013; Müller and Brandl, 2009; Noss, 1999, 1990; Tews et al., 2004). For instance, Lohbeck et al. (2015) demonstrated that biomass increment in areas undergoing secondary succession after disturbance is the main predictor of recovering ecosystem-function rates (e.g. primary productivity, litter decomposition). Our ability to successfully capture stand attributes is therefore crucial for the reliable and accurate estimation of these shifts in natural

* Corresponding author at: Amazon Environmental Research Institute (IPAM), SCN 211, bloco B, sala 201, 70836-520 Brasilia, Brazil.
E-mail addresses: barbara.zimbres@ipam.org.br (B. Zimbres), julia.shimbo@ipam.org.br (J. Shimbo), mercedes@unb.br (M. Bustamante), shaun.levick@csiro.au (S. Levick), sabrina.couto@ueg.br (S. Miranda), divino.silverio@ipam.org.br (D. Silvério), fagg@unb.br (C. Fagg), ane@ipam.org.br (A. Alencar).

https://doi.org/10.1016/j.foreco.2019.117798
Received 13 June 2019; Received in revised form 19 November 2019; Accepted 21 November 2019

ecosystems.

Traditionally, aboveground biomass (AGB) of woody vegetation has been the most frequently assessed compartment since it is easier to measure (as opposed to belowground) and since other biomass in other compartments can be derived from AGB through empirically generated expansion factors (Dixon et al., 1994). Allometric equations have been widely developed to derive estimates of aboveground biomass from measured variables, such as stem diameter, tree height, volume, and/or wood density, with relatively accurate results (e.g. Roitman et al., 2018; Alvarez et al., 2012; Feldpausch et al., 2011; Chave et al., 2005; 2014; Oliveira Filho and Scolforo, 2008; Baskerville, 1972). Such inventories are usually time consuming and cover relatively small areas. Ecological studies would highly benefit from innovative tools that allow for the measurement of vegetation structure and biomass in an accurate and timely manner, which is key for ecosystem management and monitoring at large spatial scales (Avitabile et al., 2016; Baccini et al., 2012; Saatchi et al., 2011).

More recently developed technologies can provide fast and highly accurate estimates of vegetation structure, which can be used to estimate biomass. For example, laser scanning, based on light detection and ranging (LiDAR) technology, allows for the generation of three-dimensional models of forest structure that can be subsequently related to structural attributes of interest (Lefsky et al., 2002; MacLean and Krabill, 1986; Nilsson, 1996). Three-dimensional models of forests have been generated by both air or spaceborne (ALS) and terrestrial laser scanning (TLS). The former can produce accurate models of canopy profile over large areas (Asner et al., 2012; Drake et al., 2002; Lefsky et al., 2002, 2005; Nilsson, 1996); and the latter can capture below-canopy attributes more accurately, such as understory density, stem diameter and volume, especially in more structurally complex vegetation (Chasmer et al., 2006; Côté et al., 2011; Dassot et al., 2012; Lovell et al., 2003). TLS, however, has a limited spatial footprint and some effort may be required to cover large plots. Its usefulness thus depends on whether the information gathered is accurate and more time-efficient than that obtained with classic vegetation inventories (Muir et al., 2018; Newnham et al., 2015).

The benefits of laser scanning for vegetation measurement were first explored in forestry sciences aimed at timber production, so that stem density, height and diameter at breast-height were extracted in structurally simple and relatively sparse tree stands (Dassot et al., 2011; Maclean and Krabill, 1986; Thies et al., 2004). Over the last decade the number of studies using laser scanning in natural old-growth forests for ecological investigations has increased dramatically (Levick et al., 2016; Dassot et al., 2012; Côté et al., 2011), and they have evolved to cover structurally complex and denser forests, in tropical environments (Becknell et al., 2018; Leitold et al., 2015; Longo et al., 2016; Meyer et al., 2018; Palace et al., 2016; Tanago et al., 2018). Scanning in dense vegetation is logistically challenging, and in some cases, building a mosaic of the complete plot is unfeasible, since it requires a large and time-consuming effort of placing the scanner and targets for the subsequent merging of the point clouds (Wilkes et al., 2017; Newnham et al., 2015). In some cases, working with single point clouds independently is the only efficiently way to map the structure of a complex natural stand, albeit facing the problem of occlusion by the vegetation (Palace et al., 2016). It is thus necessary to test these techniques and provide guidelines to the efficient application of laser scanning in different tropical environments, as well as understand the error associated with integrating different methodologies (e.g. Pereira et al., 2019).

Savannas are tropical formations that have been relatively little explored in terms of identifying the potential of TLS to describe vegetation structure (Béland et al., 2014, 2011) as well as to estimate aboveground biomass (Cuni-Sanchez et al., 2016; Odipo et al., 2016) and monitor structural change (Asner and Levick, 2012; Levick et al., 2015). Savannas vary widely in their structural and floristic attributes. Even at local scales, highly different vegetation types co-exist in a mosaic of formations. This is the case in the South American tropical savanna, the Cerrado biome in central Brazil, which is predominantly comprised of a typical savanna formation, while forests are found along streams or in patches, forming natural gradients of biomass across the landscape (Ribeiro and Walter, 2008). Currently, the remnant native vegetation in the Cerrado represents around 50% of the total original area (Sano et al., 2010; Beuchle et al., 2015; MapBiomas Collection 3 – www.mapbiomas.org). The Cerrado is the most structurally (and biologically) diverse savanna in the world, and most of the natural vegetation conversion is due to agricultural expansion, and tends to occur where there is dense vegetation and flat relief/corrugated plane (Rocha et al., 2011). This natural structural complexity entails highly different structural attributes and biomass stocks in different formations. It is clear that the application of LiDAR technology for biomass estimation in such complex savannas will depend on its effectiveness in capturing and describing these differences, as well as on the generation of good predictive models of aboveground biomass for each formation based on the attributes of TLS clouds.

The goal of this study was therefore to explore the potential of the terrestrial LiDAR technology to (1) capture the structural differences in three Cerrado vegetation formations that contain the largest stocks of woody biomass in the biome (woodland savanna, gallery forest, and forested savanna – *cerradão*; Brazil, MCTI, 2015) in terms of LiDAR-derived metrics; (2) generate biomass estimation algorithms based on estimates obtained from manual plot surveys; and (3) assess the impact of seasonality on biomass prediction in the highly seasonal woodland savanna. The single point clouds were our study object, and an additional methodological objective was to explore how dense should the scanning be in these different formations (how many TLS scans within a plot) to generate accurate and precise estimations of aboveground biomass.

2. Methods

2.1. Study area

Our study took place in three areas where we sampled three different Cerrado formations: 1) the Brasília Botanic Garden, Federal District, a protected area, where we sampled woodland savanna plots; 2) a ranch owned by the University of Brasilia, the Fazenda Água Limpa, Federal District, where we sampled the gallery forest plots; 3) the Fazenda Clementino, municipality of Itapirapuã, Goiás State, a privately-owned landholding where we sampled the forested savanna plots (Fig. 1). These three vegetation formations typical of the Brazilian Cerrado biome were selected for this study, because of their high proportion of woody aboveground biomass as opposed to other more open and structurally homogenous formations, as well as because of data availability from past inventories conducted at these areas. They include: (1) woodland savanna (known as cerrado *sensu stricto*), which is the typical savanna formation, comprising 61% of the native vegetation of the biome, and formed by large grass and herbaceous components as well as shrubs and trees (Sano et al., 2010); (2) a type of riparian forest, known as gallery forest, which runs along narrow streams or rivers, comprised of large and high trees whose canopies can touch over the streams, a dense understory, and the absence of the herbaceous and grass strata; and (3) the forested savanna, known as *cerradão*, which is also a forest in terms of structure (large and high trees), but includes a small grass and herbaceous strata, and is very peculiar in terms of species composition, presenting both species typical from riparian forests and woodland savanna (Ribeiro and Walter, 1998).

All sampled plots are permanent plots, where different research groups conducted field vegetation inventories, and manually collected information on diameter, height, and position of the individual trees. In the woodland savanna plots, the latest inventories were conducted in 2008, in the gallery forests in 2014, and in the forested savanna in 2017. Nonetheless, the time gap between the gallery forest and

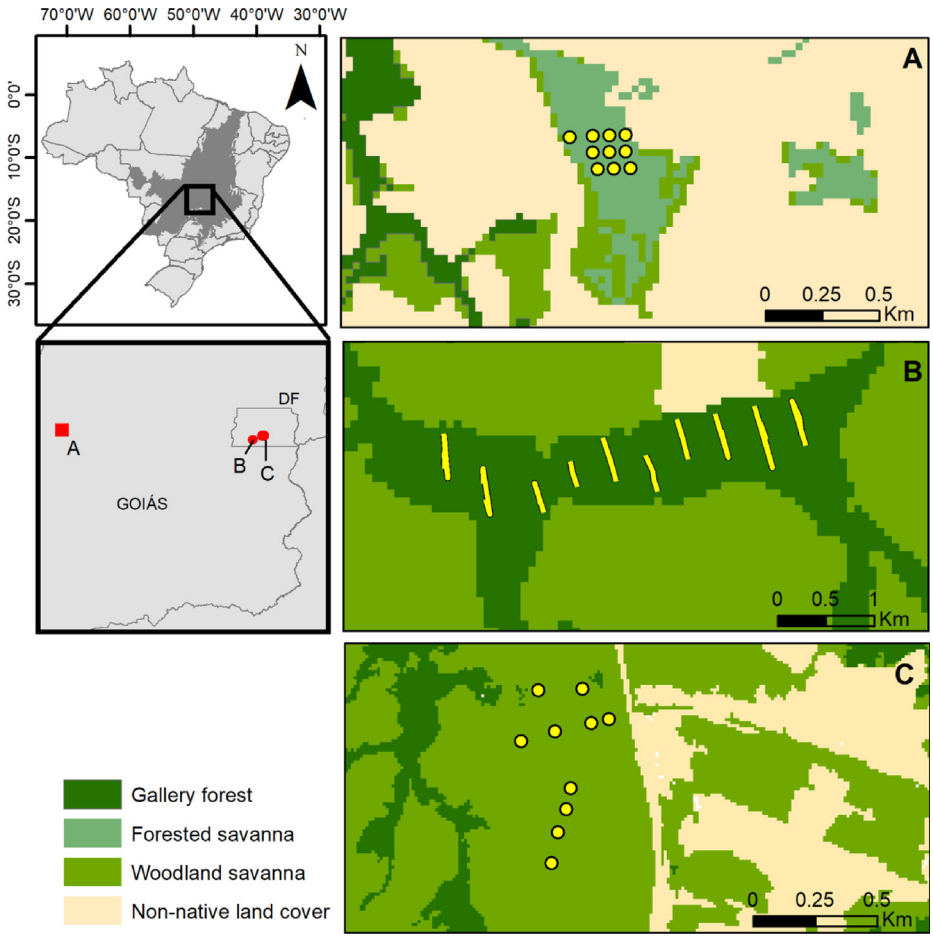

Fig. 1. Location of the study areas, and position of the scanned plots/transects, in all sampled formations: (A) forested savanna (*cerradão*), (B) gallery forest, and (C) woodland savanna (cerrado *sensu stricto*). Background land cover map adapted from MapBiomas Collection 3 (MapBiomas, 2017).

woodland savanna inventories and the TLS scanning, should have little influence in biomass estimation from the field data, since structural changes in these formations are known to be very slow, and there is no record of fire occurring in these areas during this period (Miranda, 2012; Roitman et al., 2016).

The climate in the Cerrado is classified as Köppen Aw (Peel et al., 2007), highly seasonal, with marked dry (from April to September) and rainy (from October to March) seasons (Silva et al., 2008). Mean annual precipitation varies from 1300 to 1600 (Ribeiro and Walter, 2008). The average annual temperature varies from 18 °C to 27 °C and the average annual relative humidity varies from 60 to 90% (Silva et al., 2008). The woodland savanna is semi-deciduous, with many of its trees shedding most or all of their leaves in the dry season. Deciduousness is less pronounced or absent in the forested formations.

2.2. Sampling design

The range of the utilized scanner reaches 70 m under optimal conditions, but vegetation density results in the occlusion of structural stand elements at far shorter distances than that. We conservatively observed that the scan was adequately capturing the vegetation structure within 5 m from the scan position. Therefore, in the woodland and forested savanna formations, we scanned 20 × 50-m inventory plots, divided into 10 × 10-m subplots each. Gallery forests plots, consisted of non-contiguous 10 × 20-m plots distributed along ten transects perpendicular to the forest strip, also divided into 10 × 10-m subplots. The initial sampling design therefore consisted of ten plots in the woodland and forested savanna, and four plots per transect in the gallery forest. This sampling design would have resulted in ten scans per plot in the woodland and the forested savanna, and eight scans per transect in the gallery forest. However, issues found subsequently in the field caused the exclusion of some subplots due to differences between the current structure in these subplot and the structure at the time of the inventory, for instance: a recently opened trail across the forested savanna patch affected a few of the plots, so that eight subplots were lost and could not be scanned; two subplots were excluded in the woodland savanna due to the loss of two large trees, which were inventoried but had fallen at the time of the scanning; and in one of the transects in the gallery forest, three plots were scanned instead of four, due to the narrowing of the forest strip at that specific location. Therefore, the final number of scans consisted of: 92 subplots scanned in the forested savanna (9200 m^2), 98 subplots scanned in the woodland savanna (9800 m^2), and 78 subplots in the gallery forest (7800 m^2).

Scans were taken using a FARO Laser Focus™ 70 scanner (70-m range) placed on a tripod at a height of approximately 1.5 m at the center of each subplot, working at a resolution of 12.3 mm/10 m and quality of 2x (two sample points sent in the same direction to average the position of their returns). Each scan took 3:40 min, and produced a point cloud with 11.1 million points. Each point cloud was normalized using the *lasground* and *lasheight* function in LAStools (rapidLasso, GmbH). Because point density tends to be higher close to the scanner, we applied a 2-cm voxel filter to even out the distribution of points in the cloud, using the *lidr* package (Roussel and Auty, 2019) in R 3.4.3 (R Core Team, 2017). Finally, the clouds were cropped to a 5-m radius to avoid overlap between neighboring subplots, using Fusion v. 4.80 (MacGaughey, 2018). The single point clouds were treated independently (see examples of the single point clouds in Fig. 2), and metrics were generated to describe each subplot point cloud, as

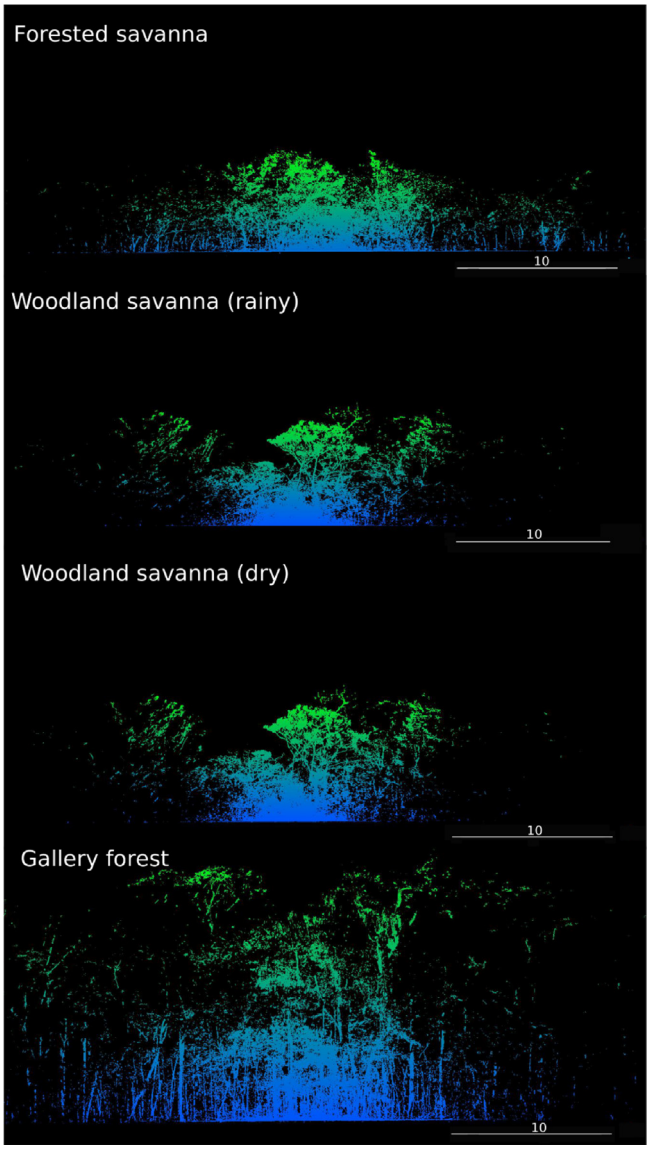

Fig. 2. Examples of point clouds obtained by scanning the vegetation of three Cerrado formations with a terrestrial laser scanner (LiDAR): forested savanna at Fazenda Clementino, Itapirapuã municipality, state of Goiás; woodland savanna in the rainy and dry seasons, at the Brasília Botanic Garden, Federal District; and gallery forest, at Fazenda Água Limpa, Brasília, Federal District, Brazil. Woodland savannas are correspondent spatially, thus depicting the temporal variation in vegetation structure at the same location.

described below.

2.3. Response variable and predictors

The response variable was the total tree aboveground biomass (AGB) estimated using allometric equations built specifically for the formations in question. These equations used manually measured height and diameter at breast height (dbh) in forests, and base diameter (db), measured at 30 cm above ground level, in the woodland savanna. The inclusion criterion considered in the inventories was db $\geq$ 5 cm in the woodland and forested savannas, and dbh $\geq$ 10 cm in the gallery forest.

The allometric equations used for generating AGB (in Mg) were specific to savanna and the specific forest formations. For the woodland savanna, the equations used was the one proposed Roitman et al. (2018), and for the forest formations, the equations used was the ones proposed by Oliveira Filho and Scolforo (2008) (SM1).

The response variable on our TLS model was the total plot AGB, which was calculated as the sum of individual tree AGB. These AGB values, obtained from the allometric models, were considered the reference values on which TLS modeling was based. Predictor variables included in the modeling were descriptive metrics of height distribution and point density per stratum, extracted from the point cloud of each subplot using Fusion v. 3.80 (MacGaughey, 2018). From the metrics produced by Fusion, we selected three variable groups that were objectively and intuitively related to vegetation density and height (Table 1). In order to generate the metric values at the plot level, height distribution and percentile variables were averaged out, and point counts per stratum were summed. We therefore highlight that mean height (Hmean) and the percentile variables cannot be interpreted as the actual mean height and height percentiles of the vegetation stand, but rather the average mean height and height percentiles taken from all subplots (Table 1).

2.4. Analyses

We tested for differences in the TLS derived metrics between formations using a one-factor analysis of variance (ANOVA). Since 16 comparisons had to be performed to test all variables among formations, we applied a Bonferroni correction to the significance value considered ($\alpha = 0.05/16 = 0.003125$). In order to assess the potential of these TLS descriptors to detect change in structure in the woodland savanna due to deciduousness, scans taken at the same location in two occasions (rainy and dry seasons) were compared through a pairwise *t* test, also applying a Bonferroni correction to the significance level considered.

Prior to modeling aboveground biomass, we conducted a manual selection of the predictors to be included in the models. The predictors were included in the model if they met the following criteria: they explained a large part of the data variance, they were not mutually colinear, and they were linearly related to the response variable. These criteria were assessed by a principal component analysis (data variance), correlation matrices (colinearity), and by individually plotting the relationships between the predictors and plot AGB. From this visual selection, up to three predictors were selected to be included in the models, due to the low number of samples in each formation (n = 10).

Modeling was then conducted at the plot-scale level, using the aggregated predictors (see Table 1) and the summed plot AGB as a response variable. Gaussian-family generalized linear models (GLM) were built for each formation separately, including all the additive combinations of the three selected predictors. First, polynomial expressions (second order) were tested against linear regressions in the case of the apparent non-linear relationships between the predictors and the response variable at the selection stage. We thus verified that all linear relationships between variables presented a better fit, so that modeling proceeded using linear regressions only. The influential variables were selected using stepwise likelihood ratio tests (Zuur et al., 2009), by comparing nested models and dropping the least significant variable (based on an F test). The final model is thus defined by the variables whose removal causes a significant decrease in the fit of the model. Residual random distribution of the final model was assessed by visual inspection.

Finally, a bootstrapping procedure was conducted in order to analyze how many subplot scans would be necessary to reach an accurate and precise estimation of plot AGB, as well as to assess the stability of coefficients of the final models. We bootstrapped different numbers of plots (from 3 to 10) with 1000 iterations, and analyzed the resulting coefficients of the modeled predictors, the adjusted R^2, and model errors (root-mean square error, or RMSE). This procedure was performed considering only the plots which had been entirely scanned (all ten subplots). The models applied to the iterations were the final models obtained in the previous analysis. We did not perform this assessment

Table 1
Descriptor variables derived from the individual point clouds, and included in the subsequent analyses as potential predictors for the modeling of aboveground biomass in the three Cerrado formations. All variables were extracted from each individual cloud, referring to the subplots within the scanned plots, and were aggregated for the overall plots using the appropriate method, described under the column Meaning.

Variable	Class	Meaning
Hmax	Height distribution	Height of highest point in all point clouds
Hmean	Height distribution	Mean of the mean point height in the point clouds
P10	Height percentile	Mean height of the 10th point distribution percentile
P20	Height percentile	Mean height of the 20th point distribution percentile
P30	Height percentile	Mean height of the 30th point distribution percentile
P40	Height percentile	Mean height of the 40th point distribution percentile
P50	Height percentile	Mean height of the 50th point distribution percentile
P60	Height percentile	Mean height of the 60th point distribution percentile
P70	Height percentile	Mean height of the 70th point distribution percentile
P80	Height percentile	Mean height of the 80th point distribution percentile
P90	Height percentile	Mean height of the 90th point distribution percentile
P99	Height percentile	Mean height of the 99th point distribution percentile
c1.37p	Point count	Total proportion of points below 1.37 m
c5p	Point count	Total proportion of points between 1.37 and 5 m
c10p	Point count	Total proportion of points between 5 and 10 m
c20p	Point count	Total proportion of points between 10 and 20 m

for the gallery forest, since we found no suitable model for this formation.

All statistical analyses were conducted in R version 3.4.3 (R Core Team, 2017), using package MuMIn (Barton, 2018).

3. Results

Basic differences of the manually measured variables between formations highlight that the gallery forest had the highest canopy, greatest trunk volumes and biomass, even with a lower density of individuals. The forested savanna was comparable to the woodland savanna in terms of basal area, and individual density. However, trees were overall shorter in the woodland savanna, which also presented the lowest levels of wood volume and biomass (Table 2).

The TLS-derived metrics successfully captured vegetation structural differences between the studied formations (Figs. 3 and 4). As expected, the gallery forest's canopy was visibly much higher than the other formations' (Hmax over three times higher in gallery forests than in the woodland savanna; Figs. 3 and 4), whereas the forested savanna was slightly taller than the woodland savanna (Hmax 50% higher; Fig. 4). Percentile-based metrics also clearly separated the forested formations from the woodland savanna, and detected differences between the gallery forest (higher) and forested savanna (lower). Point count proportions indicated that the woodland savanna had the greatest density at heights below 1.37 m (c1.37p). Despite not statistically significant, point cloud proportions at lower heights (below 1.37 and 5 m) was the most pronounced difference between seasons in the woodland savanna. The forested savanna presented the lowest density of points below 1.37 m, possibly because the tree-regeneration stratum in gallery forests is often very dense. Point count proportion between 5 and 10 m also differed between the woodland savanna and the forest formations, and, as expected, only the gallery forest presented any relevant point count proportion (up to 2.5%) at heights above 10 m (c20p).

The selection procedure used to assess data variance (SM2), collinearity (SM3-6), and the relationship between predictors and the response variable (SM7-10) resulted in the selection of three variables to be included in the modeling of AGB for the forested savanna (P20, P99, c20p); for the gallery forests and for the woodland savanna in the rainy and dry seasons (P20, P99, c1.37p).

Predictive biomass estimation models were successfully generated for the forested and woodland savannas only. No influential variables were found to predict AGB in the gallery forest, since the best model was the null model (Table 3). For the forested savanna, the final model included height of the 20th percentile (P20) (Fig. 4, Table 3), and explained 58% of AGB variance, with a RMSE of 22% (6.85 Mg/ha). There was an influence of the height of the 99th percentile (P99) and the proportion of points below 1.37 m (c1.37p) on AGB for the woodland savanna in the rainy season (Fig. 4, Table 3), with a high proportion of explained variance (adj-R^2 = 92%) and relatively low residual error (RMSE = 2.67 Mg/ha or 12%). Interestingly, c1.37p, the only variable that indicated seasonal differences in the savanna woodland, was not selected in the models for the woodland savanna in the dry season. Instead, the final model for the dry season included the height of the 99th percentile (P99) and the height of the 20th percentile (P20), with a slightly lower proportion of explained variance (adj-R^2 = 88%) and higher residual error (RMSE = 3. 23 Mg/ha or 15%) than in the rainy season (Fig. 4, Table 3).

Concerning our final study goal, the bootstrapping assessment indicated that the combination of a smaller number of scans would not result in the same level of accuracy, since the modeling considering all 10 scans produced a higher value of adj-R^2 and a smaller RMSE in all cases (Fig. 5). In fact, for the forested savanna, even considering a sampling level of nine scans per plot, the adj-R^2 values varied greatly (from 0.38 to 0.76). Interestingly, in the case of the forested savanna, the bootstrapping analyses produced a model that explained a higher amount of variance at n = 10 (adj-R^2 = 0.76) than our predictive model selection (adj-R^2 = 0.58). This discrepancy may be explained by the fact that the bootstrapping procedure could only be conducted with

Table 2
Mean (and range) of estimates of the variables obtained from the field inventories of the woody vegetation in each formation, including: basal area (BA, m^2/ha), mean tree height (Hmean, m), maximum tree height (Hmax, m), total woody volume (Volume, m^3/ha), total biomass (Biomass, Mg/ha), and total number of individuals (Nind, #/ha).

Formation	BA	Hmean	Hmax	Volume	Biomass	Nind
Forested savanna	13.0 (6.4–17.7)	5.6 (4.9–6.2)	13.1 (11.2–14.9)	100.2 (52.9–148.1)	38.3 (23.4–61.3)	1559 (640–2570)
Gallery forest	26.9 (14.8–39.4)	12.7 (12.0–13.6)	21.8 (19.0—33.0)	418.2 (211.2–656.9)	149.6 (74.5–237.4)	579.8 (437–787)
Woodland savanna	13.6 (8.6–20.7)	2.8 (2.1–3.5)	8.0 (6.0–10.0)	50.1 (230.0–98.0)	21.7 (10.1–41.8)	1884 (1550–2380)

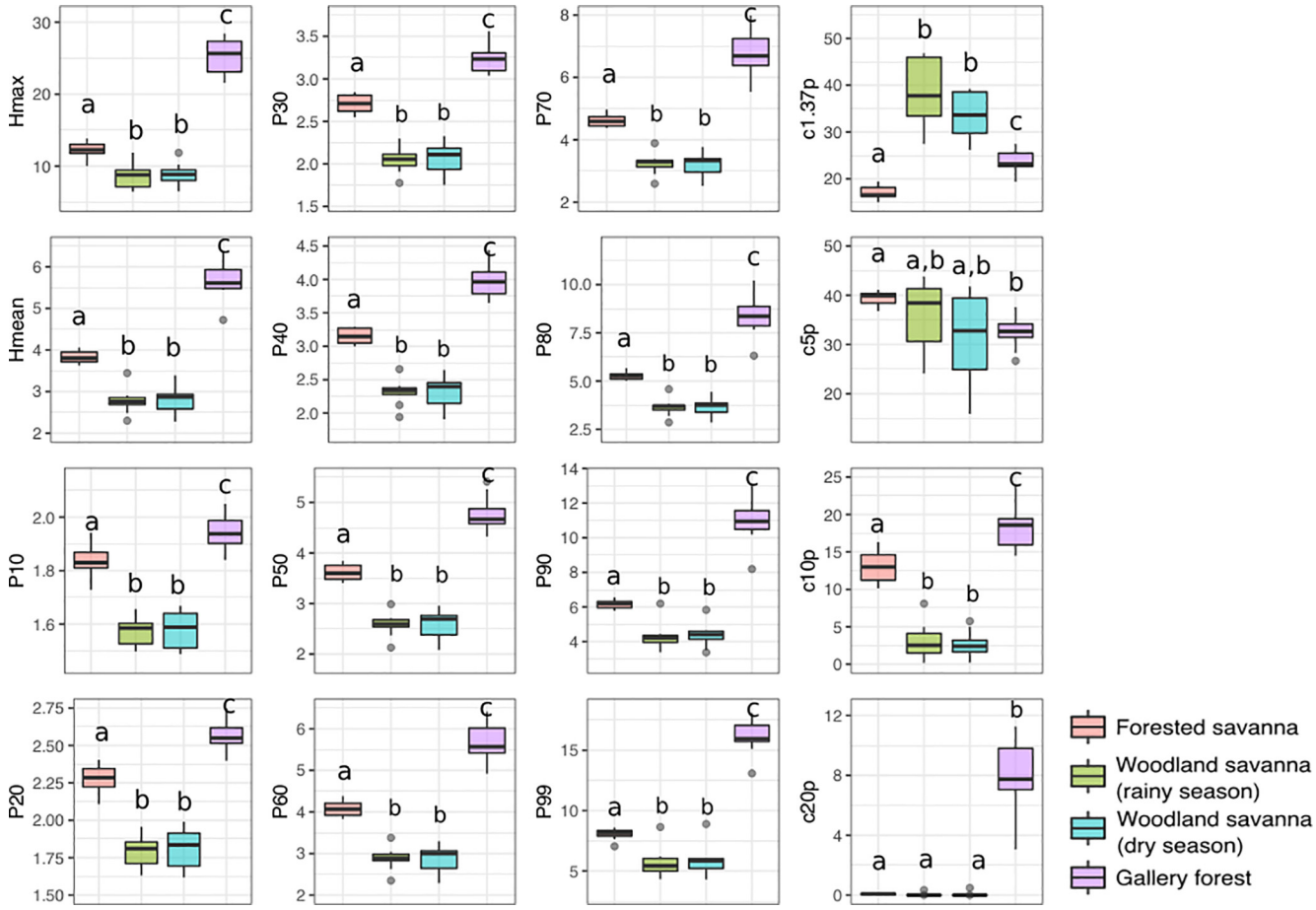

Fig. 3. Distribution of each descriptor extracted from the point clouds and aggregated by plot across all sampled formations in the Cerrado. Comparisons between different formations were conducted using a one-factor analysis of variance (ANOVA), except for the comparison between woodland savanna over the rainy and the dry seasons, which was conducted with a pairwise *t*-test. The significance level considered was $\alpha = 0.003125$, following a Bonferroni correction. TLS-derived metrics consist of: Hmax = Height of highest point in all point clouds; Hmean = Mean of the mean point height in the point clouds; P10–P99 = Mean height of the 10th–99th point distribution percentile; c1.37p = Total proportion of points below 1.37 m; c5p = Total proportion of points between 1.37 and 5 m; c10p = Total proportion of points between 5 and 10 m; and c20p = Total proportion of points between 10 and 20 m.

complete plots; that is, those plots from which a few subplots could not be scanned had to be removed from the analysis. All plots, including those 'incomplete' plots were included in the modeling procedure. When considering all plots, however, a significant drop in the RMSE could be observed, which is ultimately the goal of predictive modeling (bootstrap RMSE = 15 Mg/ha, as opposed to predictive model RMSE = 6.84 Mg/ha).

4. Discussion

4.1. TLS-based AGB estimation

AGB could be estimated with a surprisingly small number of metrics extracted from the point clouds, at least for two of the three studied formations. Plot-scale structural attributes of two formations with relatively short vegetation (up to 13 m) and open canopies (e.g. the forested and woodland savannas) could be captured using the TLS. However, the explanatory power of the models for the shorter vegetation type, the woodland savanna, was higher. An indicator of structure at the highest stratum, the height of the 99th percentile for the woodland savanna, was selected as a strong predictor of tree biomass in both seasons. However, an additional variable that contributed to the explanatory power of the models consisted in the metrics related to vegetation structure at lower heights (below 1.37 m in the rainy season, and below 2 m in the dry season). Interestingly, temporal variations in the vegetation structure for the woodland savanna were observed only at these strata. This effect is most likely related to changes underwent by the grass and shrub strata, and not by the woody vegetation, in the dry season. In the case of the rainy season, this metric was selected as a negative predictor of tree biomass, and is most likely an indicator of tree shading causing a sparser grass and shrub strata in areas with larger and taller trees. In the case of the dry season, the height of the 20th percentile (between 1.5 and 1.8 m) increases with a decrease in the density of the understory, caused, as suggested, by the same mechanism of shading of lower strata by larger trees. Therefore, in the absence of a dense grass and shrub stratum in the dry season, the effect of shading as indicator of higher woody biomass presents itself at slightly higher strata.

In the case of the forested savanna, or *cerradão*, the only selected predictor, the height of the 20th percentile, was also positively related to aboveground biomass, probably due to the same mechanism. In this case, no metric related to maximum height was selected, and the final model had a lower explanatory power than the woodland savanna. We suggest that the dense understory in the forested savanna, as well as the slightly higher vegetation, prevented the description of the structure of the highest strata at least as well as in the woodland savanna. The same appears to have occurred in describing the woody vegetation structure of the gallery forest, which could not be suitably described by the point-cloud metrics, so we were unable to generate a predictive model for AGB. This was probably because riparian forests are generally

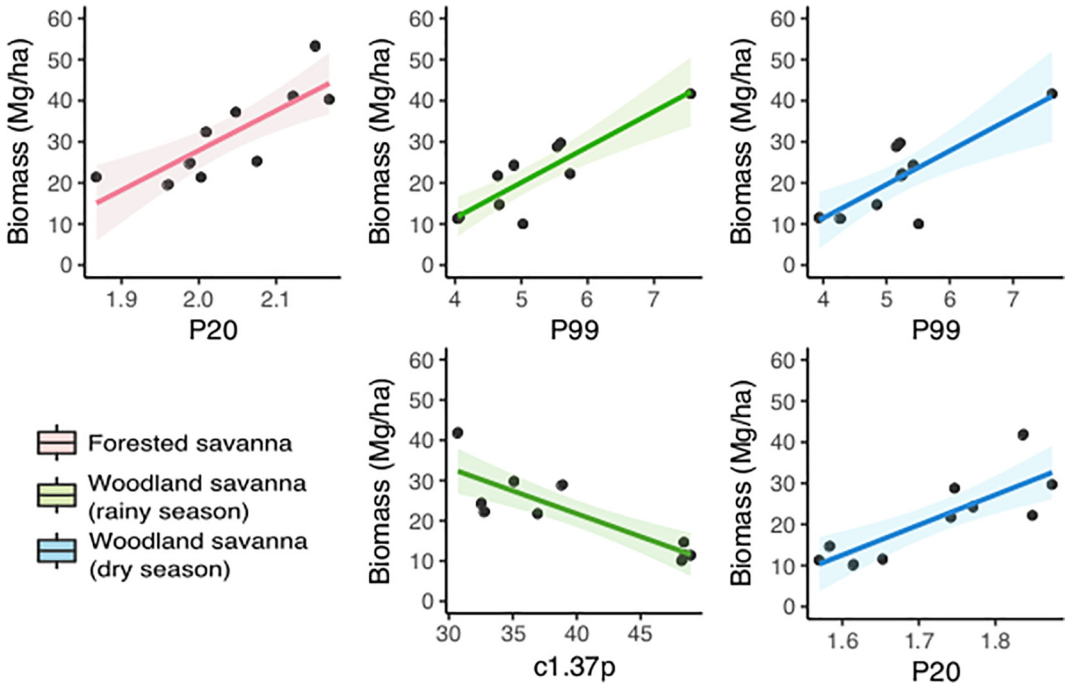

Fig. 4. Partial relationships between selected predictors and aboveground biomass in the final models obtained for the forested savanna (Fazenda Clementino, Itapirapuã municipality, state of Goiás, Brazil), and the woodland savanna in the rainy and dry seasons (Brasília Botanic Garden, Federal District, Brazil). Modeled biomass values comprise the total estimate for the entire 20 × 50-m plots.

comprised of relatively tall trees (up to 28 m) and an extremely dense understory, which prevented the scanner to generate accurate estimates of canopy structure. The discrepancy between maximum (28 m) and mean heights (4 m) observed in the gallery forest support this idea. This asymmetry in distribution indicated that most of laser points were intercepted by the dense understory, and did not reach the canopy frequently enough to generate an accurate representation of canopy structure.

Airborne LiDAR has already been shown to better delineate forest canopy structure and estimate tree height than terrestrial scanners, especially in the case of dense and tall formations (van Leeuwen and Nieuwenhuis, 2010), and our results corroborate this pattern, at least for phase-shift scanners such as the one used here. Time-of-flight TLS, with multi-return capability, may be able to penetrate and characterize the vegetation better.

4.2. Methodological considerations

Typically, and ideally, several scans are taken across a plot, and the resulting point clouds are merged to minimize occlusion and form a complete 3D model of the vegetation structure within the plot. With our scanner (FARO), the effort to merge and co-register point clouds can be quite challenging and end up being more time consuming than manual field surveys, especially in dense vegetation, where visual targets must be placed across the plot before scanning (Wilkes et al., 2017; Newnham et al., 2015), which are then used by the FARO software (Scene, 2017) to merge point clouds. Acquiring scans at single sampling stations, and averaging the resulting attributes across plots can be an efficient alternative method (Liang et al., 2016; Yao et al., 2011), but is obviously subject to the occlusion effect of the foreground objects within the plot, which will ultimately depend on the stand and understory density of the target vegetation (Olofsson and Olsson, 2018). Moreover, we can infer from the bootstrapping results that in order to

Table 3
Model comparisons according to a likelihood ratio test, conducted for each formation. A full generalized linear model (glm) of aboveground biomass (AGB) against the previously selected point cloud metrics is compared with a nested version of it, with the removal of the least influential variable in turn (results not shown). The first model which is significantly worse off after the removal of a variable is considered the final model, presented in bold font along with its significance value at the level of $\alpha = 0.05$. The generated predictive equation of AGB (in Mg/ha) for the three formation which resulted in a final model is also presented.

Formation	Models compared		df	F	p
Forested savanna	AGB ~ P20 + P99 + c20p	AGB ~ P20 + c20p	7	0.60	0.468
	AGB ~ P20 + c20p	AGB ~ P20	8	2.97	0.130
	AGB ~ P20	AGB ~ 1	9	10.89	**0.011**
	Final equation: AGB = -171.07 + 89.06*P20				
Gallery forest	AGB ~ P20 + P99 + c1.37p	AGB ~ P20 + P99	7	2.11	0.196
	AGB ~ P20 + P99	AGB ~ P99	8	3.25	0.114
	AGB ~ P99	AGB ~ 1	9	0.81	0.395
Woodland savanna (rainy season)	AGB ~ P20 + P99 + c1.37p	AGB ~ P99 + c1.37p	7	1.86	0.221
	AGB ~ P99 + c1.37p	AGB ~ P99	8	5.75	**0.047**
	Final equation: AGB = 18.78 + 4.78*P99–0.62*c1.37p				
Woodland savanna (dry season)	AGB ~ P20 + P99 + c1.37p	AGB ~ P20 + P99	7	0.11	0.755
	AGB ~ P20 + P99	AGB ~ P99	8	14.71	**0.006**
	Final equation: AGB = -71.71 + 3.92*P99 + 39.07*P20				

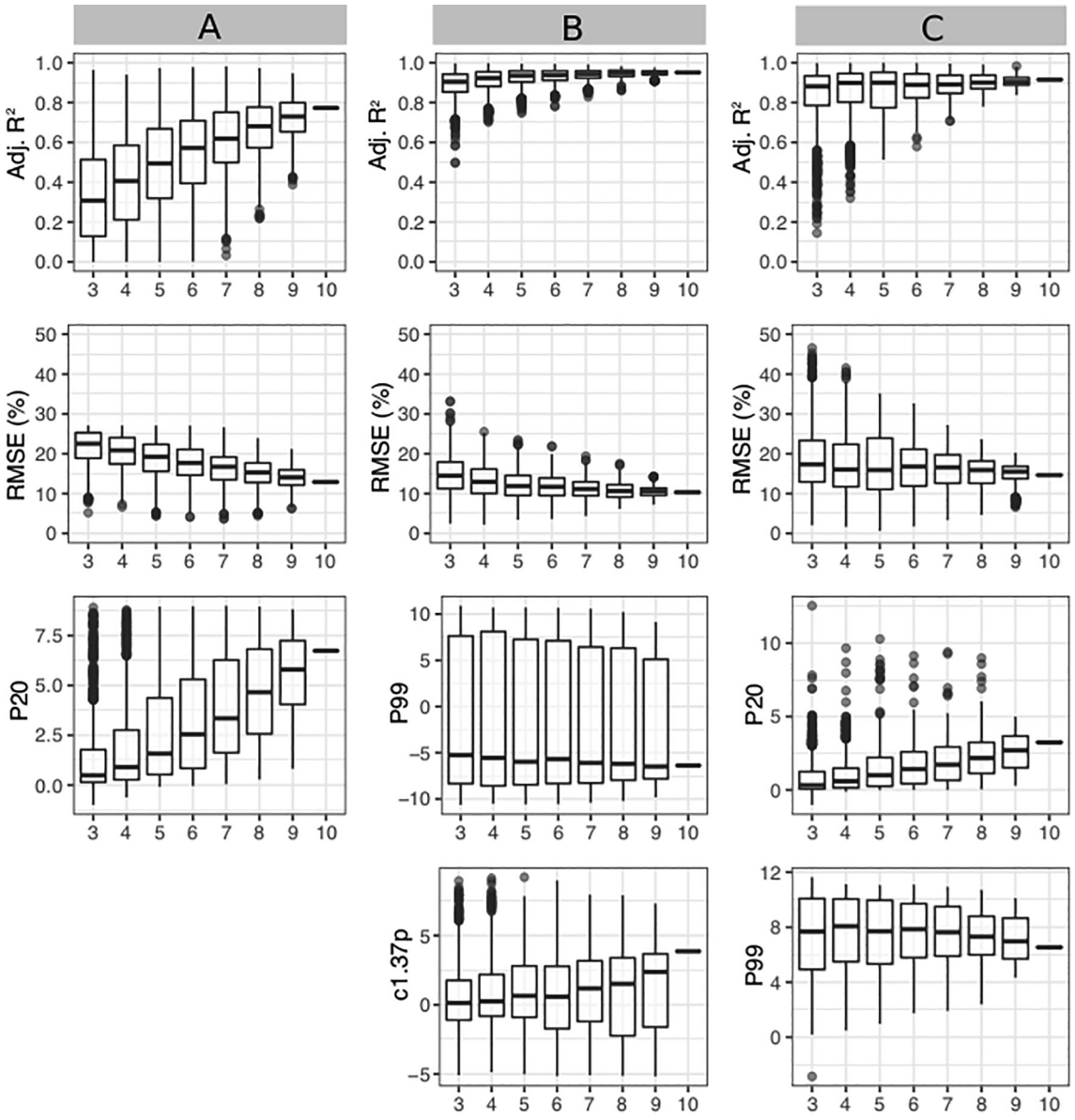

Fig. 5. Results from the bootstrapping procedure based on 1000 iterations, performed for (A) the forested savanna (Fazenda Clementino, Itapirapuã municipality, state of Goiás, Brazil), (B) the woodland savanna in the rainy season, and (C) the woodland savanna in the dry season (Brasília Botanic Garden, Federal District, Brazil), in order to assess the sufficiency of the number of single scans (one scan per subplot) to generate accurate and stable estimates for their respective models selected in the model ranking step. Model accuracy is represented by the adjusted determination coefficient (adj. R^2) and the root mean square error (RMSE). The estimated coefficients for each variable in the models are also presented.

achieve high levels of accuracy in the predictions of tree AGB, it might be necessary to place scans in a way that cover the entire plot as densely as possible to avoid occlusion, and the spacing to achieve this may be case-specific depending on stand density. This limits the time-efficiency that can be achieved using TLS for plot-scale measurements. Alternatively, advances have recently been made on the use of single scans to capture and characterize structural attributes in forest stands with the development of analytical methods that directly deal with the occlusion by foreground elements of the vegetation (Palace et al., 2016; Astrup et al., 2014; Ducey and Astrup, 2013). These techniques must be further explored.

The quality and resolution of the point clouds obtained with the LiDAR technology is outstanding, and still currently surpasses the researchers' ability to analyze and extract ecological patterns from them. The use of TLS-based metrics has been shown to be surprisingly useful, considering the time spent collecting data and the analytical simplicity. At the chosen resolution, which was satisfactorily for our purposes, an entire plot was quickly scanned (1.5 h per plot). The past surveys of the same plots, with the manually measuring of each tree individual, took approximately 6–7 h. Of course, depending on the goals of the study, manual inventories still provide a lot more information on stand attributes not accessible to laser scanners, such as species identification and the marking of individuals for long-term monitoring, and will continue to be useful.

Also, in the current approach, plot-based point cloud metrics captures features of interest somewhat indirectly. Future promising steps would be to individualize and segment trees and their main stems from the point cloud, to directly derive dbh or db as well as crown height from the point clouds (Muir et al., 2018; Olofsson and Olsson, 2018). Another promising analytical method, with the potential to improve predictive models, would be to build volume models (quantitative structural models or convex hull). For instance, in QSM, geometric forms such as cylinders or mesh surfaces are fit to the segmented tree stems and branches. This results in a geometrically-accurate three-

dimensional volume fit to each tree (Disney et al., 2018; Menaca et al., 2017; Hackenberg et al., 2014; Thies et al., 2004). However, these methods depend on the accurate 3D representation of trees from LiDAR point clouds. In complex and dense vegetation formations, such as the woodland savanna, with a dense shrubby understory and a great number of low irregular multi-stemmed trees, these techniques will be a challenge of its own. However, if this is successfully achieved, AGB estimation will surely prove to be a leap forward from manually measured estimates, or even averaged out LiDAR metrics, which still depend on the calibration using estimates from allometric models (Newnham et al., 2015). Moreover, allometric models account only for the biomass of larger trees (dbh ≥ 10 cm in the forest formations and 5 cm in the woodland savanna). Laser scanning captures the whole stand structure (all trees, shrubs, lianas, herbs, grasses). Therefore, potential and highly promising developments would involve the identification and generation of biomass models for all of these compartments.

Nevertheless, when the goal is to derive estimates of biomass over larger areas, the use of plot-based models has great potential, since it forms the base for the spatial up-scaling of predictions. Our models in the case of forested and woodland savannas have been shown to have comparable accuracies to those obtained with airborne lasers (see review by van Leeuwen and Nieuwenhuis, 2010). Firstly, plot-based scanning yields accurate estimates partly due to the averaging effect between individual scans. Secondly, terrestrial scanners give a better representation of understory structure and less dominant individuals than airborne sensors (Chasmer et al., 2006). Thus, potentially, the combination of ground-based and airborne or spaceborne (GEDI, Icesat-2) LiDAR datasets obtained over the same locations can help refine the representation of understory and canopy structure in dense formations with high levels of occlusion, such as in the case of gallery forests. Moreover, quickly retrievable, plot-based estimates from TLS may form the basis for the large-scale monitoring of biomass and carbon stocks over natural areas undergoing loss and degradation. The combination of datasets from different sources can improve tree biomass mapping by up-scaling the modeled estimates obtained over a plot to much larger areas covered by the larger-footprint sensors (Newnham et al., 2015; Zhao and Popescu, 2009). One caveat would be the need to sample more plots in order get a more complete representation of the natural variability of biomass at the original plot-scale, and, ideally, at the final scale, assessing and improving the generality of such models over a gradient of environmental conditions (van Leeuwen and Nieuwenhuis, 2010). In our case, this is a necessary next step to improve the predictive power and make use of the models generated for the Cerrado formations.

5. Conclusions

This study aimed to highlight the potential of terrestrial LiDAR technology for the generation of predictive models of plot-scale AGB, as well as for capturing and describing structural differences between different formations in Brazil's tropical savanna. In sparser formations, with relatively low trees, the ground-based scanner has corroborated this applicability, by successfully describing vegetation structure at different strata, and resulting in good predictive models, even with a low number of sampled plots. Alternately, in the galley forest (comprised of a highly dense understory), canopy heights could not be adequately characterized. In the latter case, most likely a calibration of models that associate TLS data with airborne sensors will be the solution, as well as the way to generalize and scale up predictions over larger areas. The development of such techniques will have a huge impact in our ability to map and monitor AGB and carbon stocks in the threatened Cerrado biome. Finally, we conclude that the single scan approach, with the care to cover the plots as completely as possible, can be suitable to describe vegetation structure without the need for cloud co-registration and a complete plot three-dimensional model, also at least for sparser vegetation types.

CRediT authorship contribution statement

Barbara Zimbres: Conceptualization, Methodology, Formal analysis, Writing - original draft. **Julia Shimbo:** Conceptualization, Supervision, Writing - review & editing. **Mercedes Bustamante:** Supervision, Writing - review & editing. **Shaun Levick:** Methodology, Software, Writing - review & editing. **Sabrina Miranda:** Data curation, Writing - review & editing. **Iris Roitman:** Methodology, Data curation, Investigation, Writing - review & editing. **Divino Silvério:** Methodology, Investigation, Writing - review & editing. **Leticia Gomes:** Investigation, Writing - review & editing. **Christopher Fagg:** Investigation, Data curation, Writing - review & editing. **Ane Alencar:** Supervision, Writing - review & editing.

Declaration of Competing Interest

The authors declare that they have no known competing financial interests or personal relationships that could have appeared to influence the work reported in this paper.

Acknowledgements

We are grateful to the CNPq for funding BZ's junior post-doctoral fellowship (n° 405800 2013/04), during the first year of the project. Financial support for the purchasing of the terrestrial scanner and costs for fieldwork was received from Ecometrica and the UK Space Agency's International Partnership Programme (IPP) under the Global Challenge Research Fund (GCRF). Sabrina Miranda received financial support from MCTI/CNPq/Universal 14/2014 (grant number 445420/2014-6). We are indebted to Leomar Rufino Alves Junior, Gabriel Henrique Pires de Mello Ribeiro, Waira Saravia, André Coutinho, and Gustavo Mariano Rezende for assistance in the field.

Authors' contributions

BZ, JS, MB, SL, DS, SM, and AA contributed to the study design. SM, IR, MM, and CF were responsible for the plot-based biomass inventories. BZ, JS, LG, IR, and CF conducted the fieldwork for scanning the plots using the terrestrial laser scanner. BZ processed the resulting point clouds, analyzed data, and wrote the paper, with active support from SL, DS, and JS. All authors contributed to the manuscript preparation, and approved the final manuscript.

References

Alvarez, E., Duque, A., Saldarriaga, J., Cabrera de las Salas, K.G., del Valle, I., Lema, A., Moreno, F., Orrego, S., Rodríguez, L., 2012. Tree above-ground biomass allometries for carbon stocks estimation in the natural forests of Colombia. For. Ecol. Manage. 267, 297–308. https://doi.org/10.1016/j.foreco.2011.12.013.

Asner, G.P., Levick, S.R., 2012. Landscape-scale effects of herbivores on treefall in African savannas. Ecol. Lett. 15, 1211–1217. https://doi.org/10.1111/j.1461-0248.2012.01842.x.

Asner, G.P., Mascaro, J., Muller-Landau, H.C., Vieilledent, G., Vaudry, R., Rasamoelina, M., Hall, J.S., van Breugel, M., 2012. A universal airborne LiDAR approach for tropical forest carbon mapping. Oecologia 168, 1147–1160. https://doi.org/10.1007/s00442-011-2165-z.

Asner, G.P., Powell, G.V.N., Mascaro, J., Knapp, D.E., Clark, J.K., Jacobson, J., Kennedy-Bowdoin, T., Balaji, A., Paez-Acosta, G., Victoria, E., Secada, L., Valqui, M., Hughes, R.F., 2010. High-resolution forest carbon stocks and emissions in the Amazon. Proc. Natl. Acad. Sci. 107, 16738–16742. https://doi.org/10.1073/pnas.1004875107.

Astrup, R., Ducey, M.J., Granhus, A., Ritter, T., von Lüpke, N., 2014. Approaches for estimating stand-level volume using terrestrial laser scanning in a single-scan mode. Can. J. For. Res. 44, 666–676. https://doi.org/10.1139/cjfr-2013-0535.

Avitabile, V., Herold, M., Heuvelink, G.B.M., Lewis, S.L., Phillips, O.L., Asner, G.P., Armston, J., Ashton, P.S., Banin, L., Bayol, N., Berry, N.J., Boeckx, P., de Jong, B.H.J., Devries, B., Girardin, C.A.J., Kearsley, E., Lindsell, J.A., Lopez-Gonzalez, G., Lucas, R., Malhi, Y., Morel, A., Mitchard, E.T.A., Nagy, L., Qie, L., Quinones, M.J., Ryan, C.M., Ferry, S.J.W., Sunderland, T., Laurin, G.V., Gatti, R.C., Valentini, R., Verbeeck, H., Wijaya, A., Willcock, S., 2016. An integrated pan-tropical biomass map using

multiple reference datasets. Glob. Chang. Biol. 22, 1406–1420. https://doi.org/10.1111/gcb.13139.
Baccini, A., Goetz, S.J., Walker, W.S., Laporte, N.T., Sun, M., Sulla-Menashe, D., Hackler, J., Beck, P.S.A., Dubayah, R., Friedl, M.A., Samanta, S., Houghton, R.A., 2012. Estimated carbon dioxide emissions from tropical deforestation improved by carbon-density maps. Nat. Clim. Chang. 2, 182–185. https://doi.org/10.1038/nclimate1354.
Barton, K., 2018. MuMIn: Multi-Model Inference. R package version 1.40.4.
Baskerville, G.L., 1972. Use of logarithmic regression in the estimation of plant biomass. Can. J. For. 2, 49–53.
Becknell, J.M., Keller, M., Piotto, D., Longo, M., Nara dos-Santos, M., Scaranello, M.A., Bruno de Oliveira Cavalcante, R., Porder, S., 2018. Landscape-scale lidar analysis of aboveground biomass distribution in secondary Brazilian Atlantic Forest. Biotropica 50, 520–530. https://doi.org/10.1111/btp.12538.
Béland, M., Baldocchi, D.D., Widlowski, J.L., Fournier, R.A., Verstraete, M.M., 2014. On seeing the wood from the leaves and the role of voxel size in determining leaf area distribution of forests with terrestrial LiDAR. Agric. For. Meteorol. 184, 82–97. https://doi.org/10.1016/j.agrformet.2013.09.005.
Béland, M., Widlowski, J.L., Fournier, R.A., Côté, J.F., Verstraete, M.M., 2011. Estimating leaf area distribution in savanna trees from terrestrial LiDAR measurements. Agric. For. Meteorol. 151, 1252–1266. https://doi.org/10.1016/j.agrformet.2011.05.004.
Beuchle, R., Grecchi, R.C., Shimabukuro, Y.E., Seliger, R., Eva, H.D., Sano, E.E., Achard, F., 2015. Land cover changes in the Brazilian Cerrado and Caatinga biomes from 1990 to 2010 based on a systematic remote sensing sampling approach. Appl. Geogr. 58, 116–127. https://doi.org/10.1016/j.apgeog.2015.01.017.
Blakey, R.V., Law, B.S., Kingsford, R.T., Stoklosa, J., 2017. Terrestrial laser scanning reveals below-canopy bat trait relationships with forest structure. Remote Sens. Environ. 198, 40–51. https://doi.org/10.1016/j.rse.2017.05.038.
Brazil, MCTI (Ministério da Ciência, Tecnologia e Inovação), 2015. Terceira Comunicação Nacional à Convenção-Quadro das Nações Unidas sobre Mudança do Clima. Setor Uso da Terra, Mudança do Uso da Terra e Florestas. MCTI, Brasília, Brazil, 343 pp.
Chasmer, L., Hopkinson, C., Treitz, P., 2006. Investigating laser pulse penetration through a conifer canopy by integrating airborne and terrestrial lidar. Can. J. Remote Sens. 32, 116–125. https://doi.org/10.5589/m06-011.
Chave, J., Réjou-Méchain, M., Búrquez, A., Chidumayo, E., Colgan, M.S., Delitti, W.B.C., Duque, A., Eid, T., Fearnside, P.M., Goodman, R.C., Henry, M., Martínez-Yrízar, A., Mugasha, W.A., Muller-Landau, H.C., Mencuccini, M., Nelson, B.W., Ngomanda, A., Nogueira, E.M., Ortiz-Malavassi, E., Pélissier, R., Ploton, P., Ryan, C.M., Saldarriaga, J.G., Vieilledent, G., 2014. Improved allometric models to estimate the aboveground biomass of tropical trees. Glob. Chang. Biol. 20, 3177–3190. https://doi.org/10.1111/gcb.12629.
Chave, J., Andalo, C., Brown, S., Cairns, M.A., Chambers, J.Q., Eamus, D., Fölster, H., Fromard, F., Higuchi, N., Kira, T., Lescure, J.P., Nelson, B.W., Ogawa, H., Puig, H., Riéra, B., Yamakura, T., 2005. Tree allometry and improved estimation of carbon stocks and balance in tropical forests. Oecologia 145, 87–99. https://doi.org/10.1007/s00442-005-0100-x.
Ciais, P., Sabine, C., Bala, G., Bopp, L., Brovkin, V., Canadell, J., Chhabra, A., DeFries, R., Galloway, J., Heimann, M., Jones, C., Quéré, C. Le, Myneni, R.B., Piao, S., Thornton, P., 2013. Carbon and Other Biogeochemical Cycles, in: Stocker, T.F., Qin, D., Plattner, G.-K., Tignor, M., Allen, S.K., Boschung, J., Nauels, A., Xia, Y., Bex, V., Midgley, P.M. (Eds.), Climate Change 2013: The Physical Science Basis. Contribution of Working Group I to the Fifth Assessment Report of the Intergovernmental Panel on Climate Change. Cambridge University Press, Cambridge, UK and New York, USA, pp. 465–570. https://doi.org/10.1017/CBO9781107415324.015.
Côté, J.F., Fournier, R.A., Egli, R., 2011. An architectural model of trees to estimate forest structural attributes using terrestrial LiDAR. Environ. Model. Softw. 26, 761–777. https://doi.org/10.1016/j.envsoft.2010.12.008.
Cuni-Sanchez, A., White, L.J.T., Calders, K., Jeffery, K.J., Abernethy, K., Burt, A., Disney, M., Gilpin, M., Gomez-Dans, J.L., Lewis, S.L., 2016. African savanna-forest boundary dynamics: a 20-year study. PLoS ONE 11, e0156934. https://doi.org/10.1371/journal.pone.0156934.
Dassot, M., Colin, A., Santenoise, P., Fournier, M., Constant, T., 2012. Terrestrial laser scanning for measuring the solid wood volume, including branches, of adult standing trees in the forest environment. Comput. Electron. Agric. 89, 86–93. https://doi.org/10.1016/j.compag.2012.08.005.
Dassot, M., Constant, T., Fournier, M., 2011. The use of terrestrial LiDAR technology in forest science: Application fields, benefits and challenges. Ann. For. Sci. https://doi.org/10.1007/s13595-011-0102-2.
Disney, M.I., Boni Vicari, M., Burt, A., Calders, K., Lewis, S.L., Raumonen, P., Wilkes, P., 2018. Weighing trees with lasers: advances, challenges and opportunities. Interface Focus 8, 20170048. https://doi.org/10.1098/rsfs.2017.0048.
Dixon, R.K., Brown, S., Houghton, R.A., Solomon, A.M., Trexler, M.C., Wisniewski, J., 1994. Carbon pools and flux of global forest ecosystems. Science (80-) 263, 185–190.
Ducey, M.J., Astrup, R., 2013. Adjusting for nondetection in forest inventories derived from terrestrial laser scanning. Can. J. Remote Sens. 39, 410–425. https://doi.org/10.5589/m13-048.
Drake, J.B., Dubayah, R.O., Clark, D.B., Knox, R.G., Blair, J.B., Hofton, M.A., Chazdon, R.L., Weishampel, J.F., Prince, S., 2002. Estimation of tropical forest structural characteristics, using large-footprint lidar. Remote Sens. Environ. 79, 305–319. https://doi.org/10.1016/S0034-4257(01)00281-4.
Feldpausch, T.R., Banin, L., Phillips, O.L., Baker, T.R., Lewis, S.L., Quesada, C.A., Affum-Baffoe, K., Arets, E.J.M.M., Berry, N.J., Bird, M., Brondizio, E.S., De Camargo, P., Chave, J., Djagbletey, G., Domingues, T.F., Drescher, M., Fearnside, P.M., França, M.B., Fyllas, N.M., Lopez-Gonzalez, G., Hladik, A., Higuchi, N., Hunter, M.O., Iida, Y., Salim, K.A., Kassim, A.R., Keller, M., Kemp, J., King, D.A., Lovett, J.C., Marimon, B.S., Marimon-Junior, B.H., Lenza, E., Marshall, A.R., Metcalfe, D.J., Mitchard, E.T.A., Moran, E.F., Nelson, B.W., Nilus, R., Nogueira, E.M., Palace, M., Patiño, S., Peh, K.S.H., Raventos, M.T., Reitsma, J.M., Saiz, G., Schrodt, F., Sonké, B., Taedoumg, H.E., Tan, S., White, L., Wöll, H., Lloyd, J., 2011. Height-diameter allometry of tropical forest trees. Biogeosciences 8, 1081–1106. https://doi.org/10.5194/bg-8-1081-2011.
Froidevaux, J.S.P., Zellweger, F., Bollmann, K., Jones, G., Obrist, M.K., 2016. From field surveys to LiDAR: shining a light on how bats respond to forest structure. Remote Sens. Environ. 175, 242–250. https://doi.org/10.1016/j.rse.2015.12.038.
Hackenberg, J., Morhart, C., Sheppard, J., Spiecker, H., Disney, M., 2014. Highly accurate tree models derived from terrestrial laser scan data: a method description. Forests 5, 1069–1105. https://doi.org/10.3390/f5051069.
Jenkins, D.G., 2015. Estimating ecological production from biomass. Ecosphere 6, 1–31. https://doi.org/10.1890/ES14-00409.1.
Lefsky, M.A., Harding, D.J., Keller, M., Cohen, W.B., Carabajal, C.C., Espirito-Santo, F.D.B., Hunter, M.O., de Oliveira, R., 2005. Estimates of forest canopy height and aboveground biomass using ICESat. Geophys. Res. Lett. 32, 1–4. https://doi.org/10.1029/2005GL023971.
Lefsky, M., Cohen, W.B., G.G., P., J., H.D., 2002. Lidar remote sensing for ecosystem studies. Bioscience 52, 19–30. https://doi.org/10.1641/0006-3568(2002)052[0019:LRSFES]2.0.CO;2.
Leitold, V., Keller, M., Morton, D.C., Cook, B.D., Shimabukuro, Y.E., 2015. Airborne lidar-based estimates of tropical forest structure in complex terrain: opportunities and trade-offs for REDD+. Carbon Balance Manag. 10, 1–12. https://doi.org/10.1186/s13021-015-0013-x.
Levick, S.R., Hessenmöller, D., Schulze, E.-D., 2016. Scaling wood volume estimates from inventory plots to landscapes with airborne LiDAR in temperate deciduous forest. Carbon Balance Manag. 11, 1–14. https://doi.org/10.1186/s13021-016-0048-7.
Levick, S., Setterfield, S., Rossiter-Rachor, N., Hutley, L., MacMaster, D., Hacker, J., 2015. Monitoring the distribution and dynamics of an invasive grass in tropical savanna using airborne LiDAR. Remote Sens. 7, 5117–5132. https://doi.org/10.3390/rs70505117.
Liang, X., Kankare, V., Hyyppä, J., Wang, Y., Kukko, A., Haggrén, H., Yu, X., Kaartinen, H., Jaakkola, A., Guan, F., Holopainen, M., Vastaranta, M., 2016. Terrestrial laser scanning in forest inventories. ISPRS J. Photogramm. Remote Sens. 115, 63–77. https://doi.org/10.1016/j.isprsjprs.2016.01.006.
Lohbeck, M., Poorter, L., Martínez-Ramos, M., Bongers, F., 2015. Biomass is the main driver of changes in ecosystem process rates during tropical forest succession. Ecology 96, 1242–1252. https://doi.org/10.1890/14-0472.1.
Longo, M., Keller, M., dos-Santos, M.N., Leitold, V., Pinagé, E.R., Baccini, A., Saatchi, S., Nogueira, E.M., Batistella, M., Morton, D.C., 2016. Aboveground biomass variability across intact and degraded forests in the Brazilian Amazon. Global Biogeochem. Cycles 30, 1639–1660. https://doi.org/10.1002/2016GB005465.
Lovell, J.L., Jupp, D.L.B., Culvenor, D.S., Coops, N.C., 2003. Using airborne and ground-based ranging lidar to measure canopy structure in Australian forests. Can. J. Remote Sens. 29, 607–622. https://doi.org/10.5589/m03-026.
MacGaughey, R.J., 2018. FUSION/LDV: Software for LIDAR Data Analysis and Visualization – Version 3.80. US Department of Agriculture Forest Service, Pacific Northwest Research Station.
MacLean, G.A., Krabill, W.B., 1986. Gross-merchantable timber volume estimation using an airborne lidar system. Can. J. Remote Sens. 12, 7–18. https://doi.org/10.1080/07038992.1986.10855092.
Menaca, J.G.T., Lau, A., Bartholomeusm, H., Herold, M., Avitabile, V., Raumonen, P., Martius, C., Goodman, R., Disney, M., Manuri, S., Burt, A., Calders, K., 2017. Estimation of above-ground biomass of large tropical trees with Terrestrial LiDAR. ARPN J. Eng. Appl. Sci. 12, 3218–3221. https://doi.org/10.1111/ijlh.12426.
MapBiomas Project. Collection 3 of Brazilian Land Cover & Land Use Map Series, 2017. Accessed on April 2019 (www.mapbiomas.org).
Meyer, V., Saatchi, S., Clark, D.B., Keller, M., Vincent, G., Ferraz, A., Espírito-Santo, F., d'Oliveira, M.V.N., Kaki, D., Chave, J., 2018. Canopy Area of Large Trees Explains Aboveground Biomass Variations across Nine Neotropical Forest Landscapes. Biogeosci. Discuss. 1–38. https://doi.org/10.5194/bg-2017-547.
Miranda, S.C., 2012. Variação espacial e temporal da biomassa vegetal em áreas de Cerrado Variação espacial e temporal da biomassa vegetal em áreas de Cerrado. Thesis, Universidade de Brasilia.
Muir, J., Phinn, S., Eyre, T., Scarth, P., 2018. Measuring plot scale woodland structure using terrestrial laser scanning. Remote Sens. Ecol. Conserv. https://doi.org/10.1002/rse2.82.
Müller, J., Brandl, R., 2009. Assessing biodiversity by remote sensing in mountainous terrain: the potential of LiDAR to predict forest beetle assemblages. J. Appl. Ecol. 46, 897–905. https://doi.org/10.1111/j.1365-2664.2009.01677.x.
Newnham, G.J., Armston, J.D., Calders, K., Disney, M.I., Lovell, J.L., Schaaf, C.B., Strahler, A.H., Danson, F.M., 2015. Terrestrial laser scanning for plot-scale forest measurement. Curr. For. Reports 1, 239–251. https://doi.org/10.1007/s40725-015-0025-5.
Nilsson, M., 1996. Estimation of tree heights and stand volume using an airborne Lidar system. Remote Sens. Environ. 56, 1–7. https://doi.org/10.1016/0034-4257(95)00224-3.
Noss, R.F., 1999. Assessing and monitoring forest biodiversity: a suggested framework and indicators. For. Ecol. Manage. 115, 135–146. https://doi.org/10.1016/S0378-1127(98)00394-6.
Noss, R.F., 1990. Indicators for monitoring biodiversity: a hierarchical approach. Conserv. Biol. 4, 355–364. https://doi.org/10.1111/j.1523-1739.1990.tb00309.x.
Odipo, V., Nickless, A., Berger, C., Baade, J., Urbazaev, M., Walther, C., Schmullius, C., 2016. Assessment of aboveground woody biomass dynamics using terrestrial laser scanner and L-band ALOS PALSAR data in South African Savanna. Forests 7, 294. https://doi.org/10.3390/f7120294.
Oliveira Filho, A.T., Scolforo, J.R.S., 2008. Inventário Florestal de Minas Gerais: Espécies

Arbóreas da Flora Nativa. Editora UFLA, Lavras, Brazil.
Olofsson, K., Olsson, H., 2018. Estimating tree stem density and diameter distribution in single-scan terrestrial laser measurements of field plots: a simulation study. Scand. J. For. Res. 33, 365–377. https://doi.org/10.1080/02827581.2017.1368698.
Palace, M., Sullivan, F.B., Ducey, M., Herrick, C., 2016. Estimating tropical forest structure using a terrestrial lidar. PLoS ONE 11, e0154115. https://doi.org/10.1371/journal.pone.0154115.
Peel, M.C., Finlayson, B.L., Mcmahon, T.A., 2007. Updated world map of the Koppen-Geiger climate classification. Hydrol. Earth Syst. Sci. Discuss. 4, 439–473. https://doi.org/10.5194/hess-11-1633-2007.
Pereira, I.S., Mendonça do Nascimento, H.E., Boni Vicari, M., Disney, M., DeLucia, E.H., Domingues, T., Kruijt, B., Lapola, D., Meir, P., Norby, R.J., Ometto, J.P., Quesada, C. A., Rammig, A., Hofhansl, F., 2019. Performance of laser-based electronic devices for structural analysis of Amazonian Terra-Firme Forests. Remote Sens. 11, 510.
R Core Team, 2017. R: A language and environment for statistical computing. R Foundation for Statistical Computing, Vienna, Austria.
Ribeiro, J.F., Walter, B.M., 2008. As Principais Fitofisionomias do bioma Cerrado, in: Sano, S.M., Almeida, S.P., Ribeiro, J.F. (Eds.), Cerrado: Ecologia e Flora. Embrapa Cerrados, Planaltina, pp. 151–199.
Rocha, G.F., Ferreira, L.G., Ferreira, N.C., Ferreira, M.E., 2011. Detecção de desmatamento no bioma Cerrado entre 2002 e 2009: Padrões, Tendência e Impactos. Rev. Bras. Cartogr. 63, 341–349.
Roitman, I., Bustamante, M.M.C., Haidar, R.F., Shimbo, J.Z., Abdala, G.C., Eiten, G., Fagg, C.W., Felfili, M.C., Felfili, J.M., Jacobson, T.K.B., Lindoso, G.S., Keller, M., Lenza, E., Miranda, S.C., Pinto, J.R.R., Rodrigues, A.A., Delitti, W.B.C., Roitman, P., Sampaio, J.M., 2018. Optimizing biomass estimates of savanna woodland at different spatial scales in the Brazilian Cerrado: Re-evaluating allometric equations and environmental influences. PLoS ONE 13, e0196742. https://doi.org/10.1371/journal.pone.0196742.
Roitman, I., Vanclay, J., Hay, J., Felfili, J., 2016. Dynamic equilibrium and decelerating growth of a seasonal Neotropical gallery forest in the Brazilian savanna. J. Trop. Ecol. 3, 193–200.
Roussel, J.-R., Auty, D., 2019. lidR: Airborne LiDAR Data Manipulation and Visualization for Forestry Applications. R package version 2.1.2.
Saatchi, S.S., Harris, N.L., Brown, S., Lefsky, M., Mitchard, E.T.A., Salas, W., Zutta, B.R., Buermann, W., Lewis, S.L., Hagen, S., Petrova, S., White, L., Silman, M., Morel, A., 2011. Benchmark map of forest carbon stocks in tropical regions across three continents. Proc. Natl. Acad. Sci. 108, 9899–9904. https://doi.org/10.1073/pnas.1019576108.
Sano, E.E., Rosa, R., Brito, J.L.S., Ferreira, L.G., 2010. Land cover mapping of the tropical savanna region in Brazil. Environ. Monit. Assess. 166, 113–124. https://doi.org/10.1007/s10661-009-0988-4.
Scene (version 7.0.2.5.), 2017. FARO Technologies Inc.
Silva, F.M., Assad, E.D., Evangelista, B.A., 2008. Caracterização climática do Bioma Cerrado. In: Sano, S.M., Almeida, S.P., Ribeiro, J.P. (Eds.), Cerrado: Ecologia e Flora. Embrapa, Planaltina, pp. 69–88.
Tanago, J.G., Lau, A., Bartholomeus, H., Herold, M., Avitabile, V., Raumonen, P., Martius, C., Goodman, R.C., Disney, M., Manuri, S., Burt, A., Calders, K., 2018. Estimation of above-ground biomass of large tropical trees with terrestrial LiDAR. Methods Ecol. Evol. 9, 223–234. https://doi.org/10.1111/2041-210X.12904.
Tews, J., Brose, U., Grimm, V., Tielbörger, K., Wichmann, M.C., Schwager, M., Jeltsch, F., 2004. Animal species diversity driven by habitat heterogeneity/diversity: the importance of keystone structures. J. Biogeogr. 31, 79–92. https://doi.org/10.1046/j.0305-0270.2003.00994.x.
Thies, M., Pfeifer, N., Winterhalder, D., Gorte, B.G.H., 2004. Three-dimensional reconstruction of stems for assessment of taper, sweep and lean based on laser scanning of standing trees. Scand. J. For. Res. 19, 571–581. https://doi.org/10.1080/02827580410019562.
van Leeuwen, M., Nieuwenhuis, M., 2010. Retrieval of forest structural parameters using LiDAR remote sensing. Eur. J. For. Res. 129, 749–770. https://doi.org/10.1007/s10342-010-0381-4.
Vilà, M., Carrillo-Gavilán, A., Vayreda, J., Bugmann, H., Fridman, J., Grodzki, W., Haase, J., Kunstler, G., Schelhaas, M.J., Trasobares, A., 2013. Disentangling biodiversity and climatic determinants of wood production. PLoS ONE 8, e53530. https://doi.org/10.1371/journal.pone.0053530.
Wilkes, P., Lau, A., Disney, M., Calders, K., Burt, A., Gonzalez de Tanago, J., Bartholomeus, H., Brede, B., Herold, M., 2017. Data acquisition considerations for Terrestrial Laser Scanning of forest plots. Remote Sens. Environ. 196, 140–153. https://doi.org/10.1016/j.rse.2017.04.030.
Yao, T., Yang, X., Zhao, F., Wang, Z., Zhang, Q., Jupp, D., Lovell, J., Culvenor, D., Newnham, G., Ni-Meister, W., Schaaf, C., Woodcock, C., Wang, J., Li, X., Strahler, A., 2011. Measuring forest structure and biomass in New England forest stands using Echidna ground-based lidar. Remote Sens. Environ. 115, 2965–2974. https://doi.org/10.1016/j.rse.2010.03.019.
Zhao, K., Popescu, S., 2009. Lidar-based mapping of leaf area index and its use for validating GLOBCARBON satellite LAI product in a temperate forest of the southern USA. Remote Sens. Environ. 113, 1628–1645.
Zuur, A., Ieno, E., Walker, N., Saveliev, A., Smith, G., 2009. Mixed Effects Models and Extensions in Ecology with R. Springer, New York.